Received 4 July 2023; revised 19 August 2023; accepted 21 August 2023. Date of publication 24 August 2023; date of current version 7 September 2023.
The review of this article was arranged by Editor S. Ikeda.

Digital Object Identifier 10.1109/JEDS.2023.3308368

A Low-Cost Passivation for Low Temperature Cu-Cu Bonding Using PVD-Deposited Cu_3N

TZU-HENG HUNG[1], PING-JUNG LIU[2], CHIAO-YEN WANG[1], TSAI-FU CHUNG[3], AND KUAN-NENG CHEN[1,2] (Fellow, IEEE)

1 Institute of Electronics, National Yang Ming Chiao Tung University, Hsinchu 30010, Taiwan
2 International College of Semiconductor Technology, National Yang Ming Chiao Tung University, Hsinchu 30010, Taiwan
3 Department of Materials Science and Engineering, National Yang Ming Chiao Tung University, Hsinchu 30010, Taiwan

CORRESPONDING AUTHOR: K.-N. CHEN (e-mail: knchen@nycu.edu.tw)

This work was supported in part by the "Center for the Advanced Semiconductor Technology Research" from the Featured Areas Research Center Program within the framework of the Higher Education Sprout Project by the Ministry of Education (MOE), Taiwan, and in part by the National Science and Technology Council, Taiwan, under Grant NSTC 111-2634-F-A49-008-, Grant NSTC 112-2221-E-A49-163-MY3, and Grant NSTC 110-2221-E-A49-086-MY3.

ABSTRACT PVD-deposited Cu_3N has been demonstrated for Cu-Cu bonding as a low-cost passivation material. Cu_3N exhibits stability at room temperature but undergoes decomposition upon heating, making it an attractive candidate for Cu bonding passivation. XRD analysis reveals that the decomposition of PVD-deposited Cu_3N primarily occurs within the temperature range of 200°C∼250°C. Cu_3N-Cu_3N bonding, relying on the decomposition reaction, is successfully demonstrated, and TEM analysis confirms the presence of Cu grains at the bonding interface. Moreover, Cu bonding using Cu_3N passivation has been demonstrated as well. The bonding capability at low temperatures is found to be influenced by the thin film properties of Cu_3N. For wafer level bonding, the N_2 flow rate during Cu_3N deposition requires careful adjustment to balance the anti-oxidation capability and the N_2 outgassing phenomenon. For chip level bonding, the N_2 outgassing phenomenon poses no significant issue. By demonstrating the potential of Cu_3N as a passivation material, this study suggests a promising method for achieving lower temperature requirements in Cu bonding through the adjustment of Cu_3N thin film properties.

INDEX TERMS Copper nitride, Cu bonding, passivation technology, PVD-deposited Cu_3N.

I. INTRODUCTION

With the tremendous development of AI applications and the increasing demand for high-performance computing (HPC), the significance of advanced packages has raised in recent years. Advanced package technologies offer an alternative path from transistor scaling to enhance the performance of electron devices. As a result, numerous institutes and companies have engaged in this field, including EMIB from Intel [1], [2], SoIC from TSMC [3], [4], and etc. In advanced package schematics, the transmission distance of signal and power among functional chiplets could be significantly reduced. This reduction alleviates the RC delay issue and improves power signal integrity. To properly connect these chiplets, the bonding technique plays a crucial role. For stacked chiplets, the structure must possess robust mechanical strength and high-quality electrical paths. While the mechanical strength could be provided by dielectric bonding under 200°C [5], [6], to achieve good bonding quality with conventional Cu metal interconnects, requires a temperature over 300°C for Cu oxides dissolution [7]. However, such high temperatures can degrade the devices and thus impact the feasibility of this technique [8], [9]. Consequently, many researchers have focused on the approaches to achieve excellent Cu-Cu bonding within a lower thermal budget.

In low temperature Cu-Cu bonding methods, passivation technology proves to be an effective approach for reducing native Cu oxides by creating a protective passivation layer that facilitates Cu atom diffusion. The selection of the passivation layer offers various options with different properties. For example, the self-assembled monolayer (SAM) technique employs organic passivation materials that require removal prior to Cu-Cu bonding [10], [11]. The effectiveness of Cu-Cu bonding using the SAM technique depends

This work is licensed under a Creative Commons Attribution-NonCommercial-NoDerivatives 4.0 License. For more information, see https://creativecommons.org/licenses/by-nc-nd/4.0/

on the anti-oxidation capability and the cleaning conditions of the organic passivation material. On the other hand, metal can serve as a passivation material eliminating the need for removal due to its conductive properties. Noble metals such as Au, Ag, or Pt are particularly suitable as passivation materials [12], [13], [14], because they are less prone to oxidation and can realize Cu-Cu bonding even at the temperature less than 100°C. However, the use of noble metals in the Back-End-of-Line (BEOL) is not common and can increase process cost. Therefore, it is essential to find lower-cost passivation material.

In this study, PVD-deposited copper nitride (CuN) as a cost-effective passivation material has been proposed. CuN, applied as a surface protection layer, has been reported using a two-step plasma treatment method and demonstrated blanket Cu-Cu bonding at 260°C [15], [16]. It has been proposed that CuN exhibits stability at room temperature but decomposes into Cu and N_2 when heated [17], [18], [19]. These characteristics make CuN suitable for protecting Cu from oxidation and achieving good Cu-Cu joint during the bonding process. However, the formation of CuN through plasma treatment can cause changes in the step height for Cu/SiO_2 hybrid bonding [20], which poses challenges in achieving optimal bonding results. Thus, the potential of PVD-deposited CuN as a passivation material for low temperature Cu-Cu bonding has been examined.

II. PROCESS FLOW

In order to investigate the impact of CuN as a passivation metal on Cu-Cu bonding, two different test vehicle structures were employed in this study. The first structure involved a thin CuN layer on top of Cu, representing a typical metal-passivated Cu-Cu bonding approach. In contrast, the second structure replaced the entire Cu layer with a thick CuN layer. This configuration aimed to examine the behavior of PVD-deposited CuN before and during the bonding process. The fabrication of the test vehicles followed a 4-inch wafer process, as illustrated in Fig. 1. Firstly, standard RCA clean was performed on 4-inch Si wafers. Next, a 500 nm SiO_2 layer was deposited on the surface through thermal oxidation. The sequential metal deposition processes were carried out using a sputtering system (DC-sputtering, Ion Tech Microvac 450CB). For the test vehicle with a thin copper nitride condition, the layer consisted of 30 nm Ti, 300 nm Cu, and 10 nm CuN. For the thick copper nitride condition, the layer included 30 nm Ti and 100 nm CuN. The structural schematics are depicted in Fig. 2. The working pressure during metal deposition was about 1 Pa. For Ti deposition, the DC power was set to 140 W, with an Ar flow rate of 24 sccm. For Cu deposition, the DC power was 130 W, and the Ar flow rate was 24 sccm. CuN deposition used the same Cu target as Cu deposition, but with a gas mixture of N_2 and Ar. Three different flow rate ratios were employed in this study, denoted as 30%-CuN. 50%-CuN and 80%-CuN, with the gas flow rates detailed in Table 1.

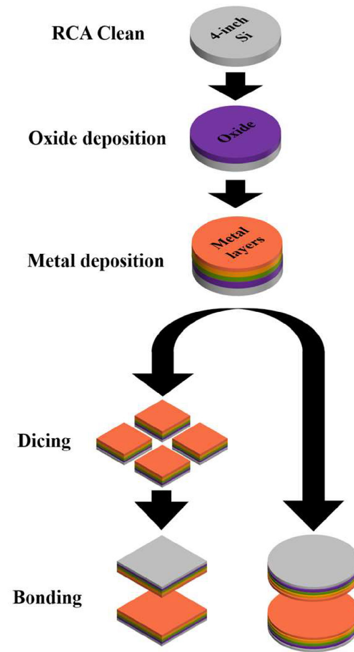

FIGURE 1. The process flow for both thin CuN passivation and thick CuN specimens.

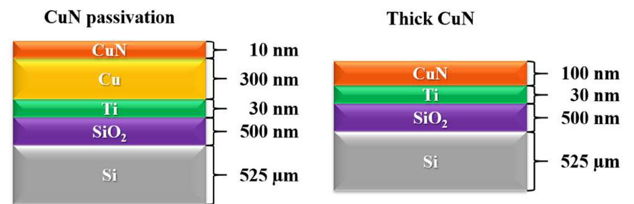

FIGURE 2. The structure schematics of thin CuN passivation specimen and thick CuN specimen.

TABLE 1. Flow rate during CuN PVD process.

	30%-CuN	50%-CuN	80%-CuN
N_2 flow rate	7.2 sccm	12 sccm	19.2 sccm
Ar flow rate	16.8 sccm	12 sccm	4.8 sccm

To examine the properties of the thin film, X-ray diffraction (XRD) analysis was performed to determine the crystallization condition of the PVD-deposited CuN and any changes that occurred after heating the CuN film. In the case of thin CuN passivation, where the CuN layer on top of the Cu layer is only around 10 nm thick, the XRD signals primarily captured the signal from the Cu layer, resulting in a spectrum dominated by Cu. X-ray photoelectron spectroscopy (XPS) depth analysis was conducted to investigate the element composition and oxidation condition of the test vehicle. Atomic force microscopy (AFM) analysis was utilized to assess the surface roughness of the test vehicles prior to bonding. Besides, a four-point probing system was employed to measure the sheet resistance of each metal stacking structure.

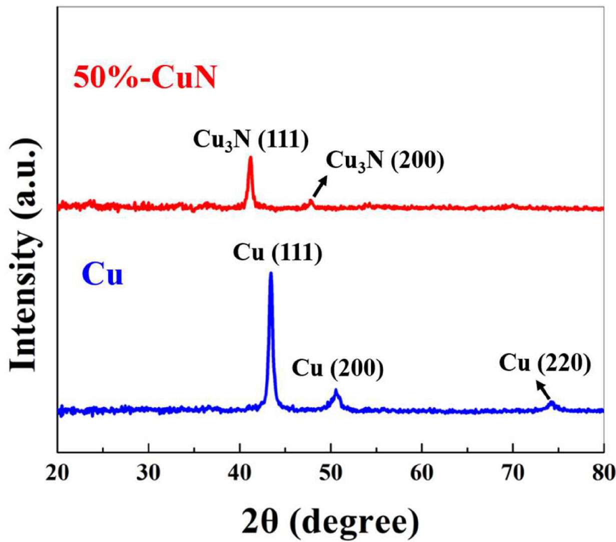

FIGURE 3. XRD results of 50%-CuN and Cu.

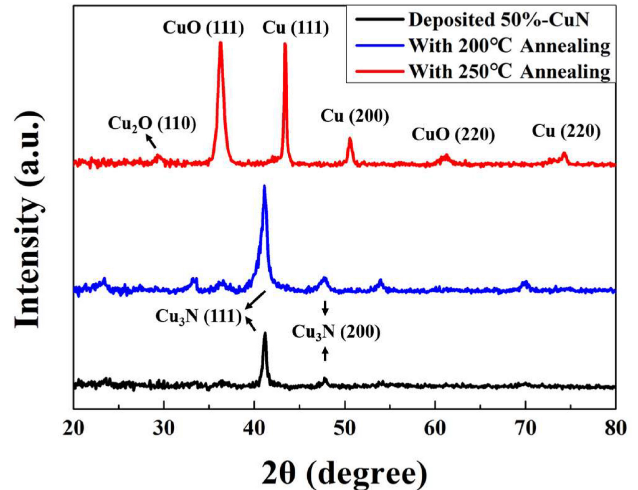

FIGURE 4. XRD results of deposited 50%-CuN, 50%-CuN with 200°C annealing and 50%-CuN with 250°C annealing.

The thermal compression bonding (TCB) process was carried out at both chip level and wafer level. For wafer level bonding (Aligner wafer bonder, AWB-08), the two wafers were bonded under a vacuum environment of 10^{-4} Torr at 250°C. The bonding pressure was approximately 1.30 MPa, and the bonding duration was set to 50 minutes. In the case of flip-chip bonding (SET, ACCμRA 100), the test vehicles were diced into sizes of 10 x 10 mm and 15 x 15 mm as the top chips and bottom chips, respectively, in advance. The two chips were bonded at atmosphere with a bonding force of 80 kgf. The bonding temperature was set to 250°C and the bonding duration was 6 minutes.

To assess the bonding quality and investigate the bonding mechanism of the PVD-deposited CuN as the passivation metal for Cu-Cu bonding, several analyses were performed. Scanning acoustic tomography (SAT) analysis was utilized to detect the presence of bonding voids larger than 5 μm at the bonding interface. Pull tests were used to measure the mechanical strength of the bonding interface under external forces applied in the normal direction. Additionally, to unravel the bonding mechanism, bonded test vehicles were prepared using focused ion beam (FIB) for transmission electron microscope (TEM) (JOEL, JEM-2010F) and energy-dispersive X-ray spectroscopy (EDS) analyses.

III. RESULTS AND DISCUSSION

A. THICK CuN

The thick 50%-CuN specimen was inspected by XRD analysis, as shown in Fig. 3, to determine its crystallization condition. The presence of Cu_3N (111) orientation, along with a small amount of Cu_3N (200), was observed in the XRD spectrum for the thick CuN structure. This confirms that the deposited CuN exhibits Cu_3N crystallization. In Fig. 3, the Cu specimen consists of a 30 nm Ti and a 300 nm Cu, which is identical to the CuN passivation structure with only the addition of a CuN layer. For the comparison, the XRD results reveals that the deposited Cu film primarily exhibits Cu (111) orientation, with some occurrences of Cu (200) and Cu (220).

Next, the decomposition behavior of the PVD-deposited Cu_3N was investigated through annealing at different temperatures. The decomposition reaction of Cu_3N can be represented by the following equation [19]:

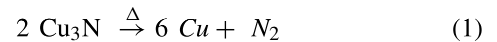

$$2\ Cu_3N \overset{\Delta}{\rightarrow} 6\ Cu + N_2 \quad (1)$$

Upon heating, Cu_3N undergoes decomposition into Cu and N_2. In order to analyze the changes in crystallization condition, the focus of the examination was on the thick CuN specimen. This is because the crystallization results of the CuN passivation specimen would be dominated by the Cu peaks, even without further annealing, due to the only 10 nm thinness of the CuN layer. The conducted annealing temperatures are 200°C and 250°C, respectively. The annealing duration is 1 hour and the process is done at vacuum under 10^{-4} Torr in each case. The XRD analysis results are presented in Fig. 4. The XRD analysis indicates that the Cu_3N signal degraded after annealing at 200°C, suggesting partial decomposition of the Cu_3N crystals. With the 250°C annealing, the spectrum is dominated by Cu and Cu oxides, indicating extensive decomposition of Cu_3N into Cu, accompanied by an oxidation reaction. Based on these results, it can be inferred that the decomposition reaction of PVD-deposited CuN significantly occurs between 200°C and 250°C. Consequently, a bonding temperature of 250°C was selected for both CuN passivation bonding and thick CuN bonding to utilize the decomposition reaction.

Following chip-level bonding for thick 50%-CuN, the bonding interface was examined through TEM analysis, as depicted in Fig. 5. Fig. 5(a) presents the dark field cross-sectional image of the bonding interface. It demonstrates a well-bonded interface between the two CuN layers. Moreover, bright spots can be observed at the bonding

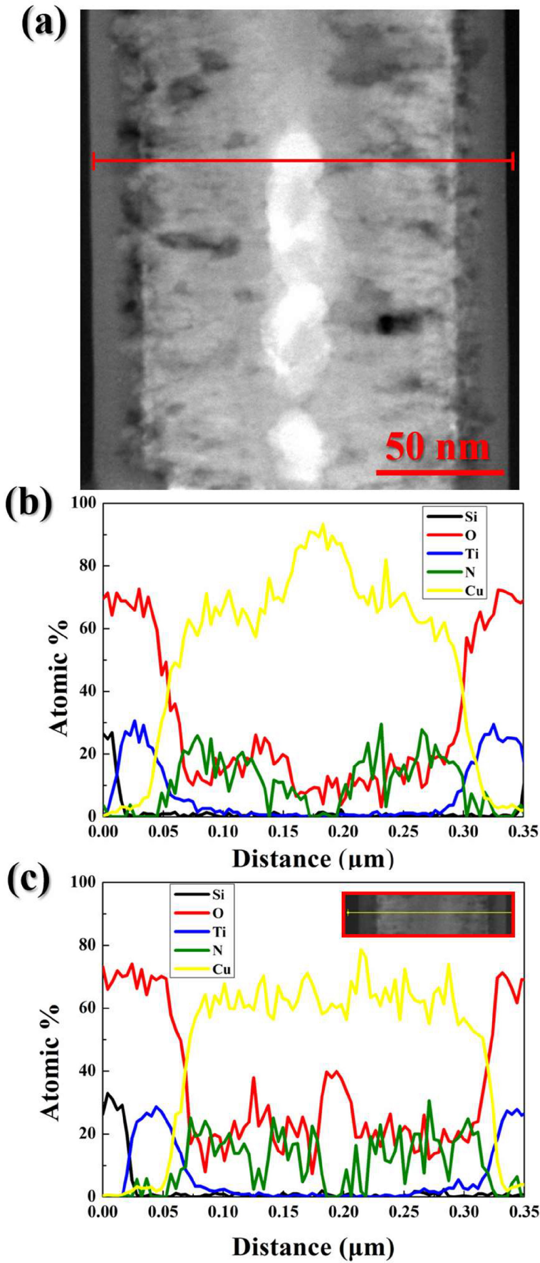

FIGURE 5. (a) TEM image of bonded thick 50%-CuN specimen with the red line indicating EDX scan region. (b) EDX line scan result crossing the bonding interface with bright spots. (c) EDX line scan result crossing the bonding interface with no bright spots.

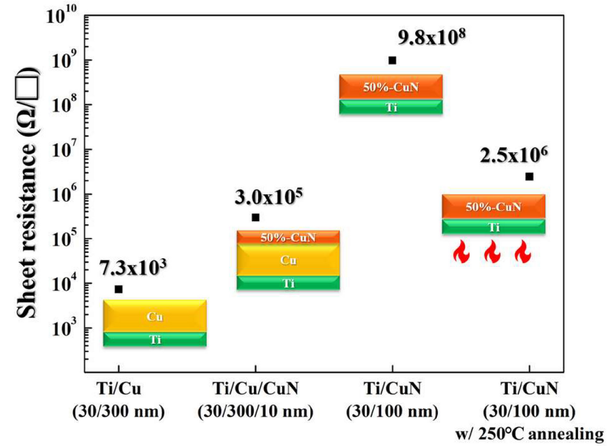

FIGURE 6. Sheet resistance result of Cu, CuN passivation, and thick CuN with and without 250°C annealing for 50 minutes.

interface, suggesting regions with varying elemental compositions. The red line in the image indicates the scanned region of EDX analysis, and the corresponding results are illustrated in Fig. 5(b).

In Fig. 5(b), the composition line-scanning was conducted across the Ti/CuN/CuN/Ti bonding structure, revealing bright spots at the bonding interface. Notably, an evident increase in the Cu atomic ratio was observed at the bonding interface, accompanied by a decrease in the N atomic ratio to near 0%. This finding aligns with the XRD analysis, indicating an obvious decomposition reaction taking place in the Cu_3N film. Furthermore, the TEM results demonstrate that this decomposition reaction plays a beneficial role in the bonding process. The formation of Cu at the bonding interface facilitates the connection between the bonded pair.

In contrast, the EDX line-scanning result across the bonding interface without bright spots is shown in Fig. 5(c). The insertion in Fig. 5(c) is a cross-sectional image, with a yellow line indicating the scanned region. In contrast to the previous result, the atomic ratio of Cu does not exhibit an increase. However, the atomic ratio of O becomes higher, accompanied by a decrease in the N ratio. This phenomenon is observed in wafer-level bonding as well. Considering the vacuum environment during the wafer bonding process, it is more likely that the increased oxygen is derived from surface adsorption/absorption prior to bonding, as no additional pretreatment process was conducted for surface cleaning.

While the bonding ability of the 100 nm CuN film under 250°C has been demonstrated, it is important to consider the potential impact of CuN on the electrical performance of the metal joint. Fig. 6 presents the results of the sheet resistance measurements for each metal stacking structure. In the case of 50%-CuN, even a thin 10 nm passivation layer leads to an increase in sheet resistance compared to a Cu film without passivation. Replacing the 300 nm Cu film with a 100 nm 50%-CuN film results in a sheet resistance that becomes five orders higher. Although the decomposition of CuN into Cu can reduce the sheet resistance, the presence of non-decomposed CuN can adversely affect the electrical performance of the metal contact [21]. As depicted in Fig. 6, the sheet resistance of thick CuN structure would be reduced by two orders after annealing at 250°C annealing for 50 minutes under 10^{-4} Torr. However, the sheet resistance of the annealed thick CuN structure is still high, which might be because of insufficient decomposition or Cu oxidation. Therefore, using a CuN passivation layer to cover the Cu surface appears to be a more favorable approach than completely replacing the bonding structure with CuN.

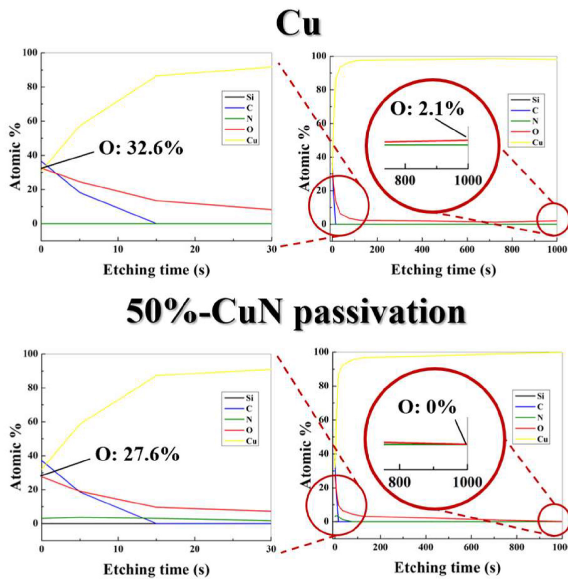

FIGURE 7. XPS depth analysis results of Cu and 50%-CuN after three weeks storage.

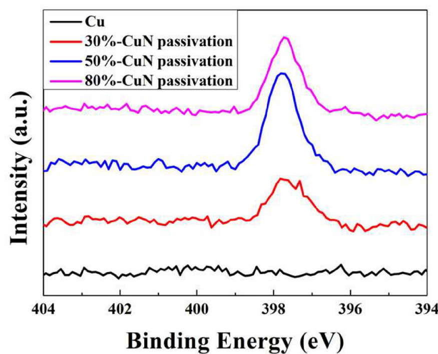

FIGURE 8. N1s spectrum of Cu, 30%-CuN, 50%-CuN, and 80%-CuN.

B. CUN PASSIVATION

Fig. 7 illustrates the oxidation condition of Cu and Cu with 50%-CuN passivation. Both specimens were stored under the same conditions in a clean room environment at room temperature for three weeks. Surface contamination was observed in both specimens, with the presence of carbon and oxygen elements alongside Cu or nitride. The carbon signal profiles exhibited similar values in both examinations, suggesting similar particle conditions. However, the oxygen profile showed a slightly lower element percentage in the 50%-CuN passivation specimen compared to the Cu specimen. More significantly, the oxygen percentage remained consistently throughout the Cu film in the Cu specimen, whereas in the 50%-CuN passivation specimen, the oxygen percentage gradually decreased to zero within its Cu film region. These results indicate that the use of a thin PVD-deposited CuN passivation layer helps alleviate the oxidation phenomenon.

Fig. 8 presents the N1s spectrum analysis by XPS, with the deposition conditions corresponding to the 30%-, 50%-, and 80%-CuN specimens as outlined in Table 1. In the N1s spectrum, no distinct peak is observed for the Cu specimens. However, for the CuN passivation specimens, a clear peak near 397.28 eV is detected. This peak corresponds to the CuN bond, as indicated in the literature [16], confirming the formation of CuN through the PVD deposition method, consistent with the XRD results for the thick CuN specimen in Fig. 3. Furthermore, the CuN peak in the N1s spectrum appears weaker for the 30%-CuN passivation compared to the 50%- and 80%-CuN specimens. This could be attributed to an insufficient N_2 flow rate during deposition.

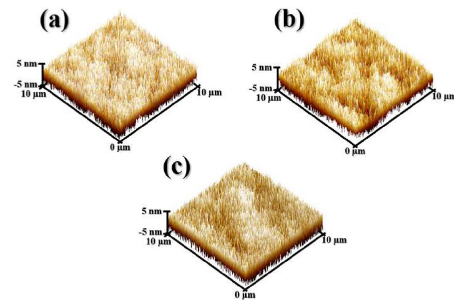

FIGURE 9. Surface roughness results of 30%-CuN, 50%-CuN, and 80%-CuN.

Fig. 9 shows the surface roughness measurements for 30%-, 50%-, and 80%-CuN passivation specimens, with respective root mean square roughness (R_q) values of 2.15 nm, 1.84 nm and 2.10 nm. These values suggest that the change in flow rate composition during the deposition process does not have a significant impact on the surface topography of CuN. Furthermore, the smooth surface with nanometer-scale flatness observed in all three specimens is advantageous for achieving high-quality bonding.

The results of the bonding quality inspection for wafer level Cu-Cu bonding with thin PVD-deposited CuN passivation are presented in Fig. 10. Fig. 10(a) and Fig. 10(b) show the SAT images of the 30%- and 50%-CuN passivation specimens, respectively. Under a bonding temperature of 250°C, the 50%-CuN passivation yields good bonding quality, as observed in Fig. 10(b). However, the bonding quality for the 30%-CuN passivation, as shown in Fig. 10(a), appears to be poor. This poor bonding quality is unlikely to be caused by the outgassing issue from CuN decomposition, as the XPS result indicates weaker CuN bond formation for the 30%-CuN passivation compared to the 50%-CuN passivation. Instead, it is more likely attributed to Cu oxidation, as insufficient CuN coverage fails to provide adequate protection against oxidation. On the other hand, the 80%-CuN passivation specimen could not be successfully bonded under the same bonding conditions, possibly due to severe outgassing, which hampers the bonding of decomposed Cu atoms between the two wafers. Fig. 10(c) shows the pull test results of bonded Cu, 30%-CuN passivation and 50%-CuN passivation specimens. It can be observed that, with proper deposition condition, PVD-deposited CuN as a

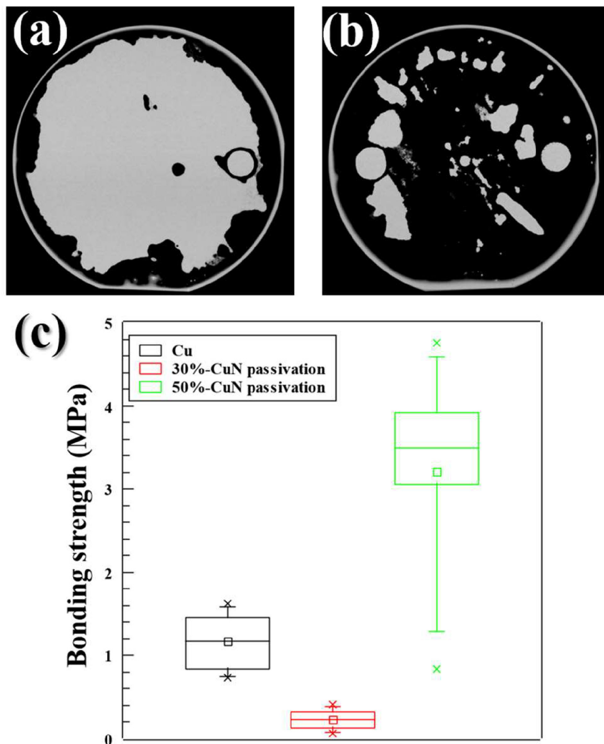

FIGURE 10. (a) SAT image of 30%-CuN bonded wafer pair, (b) SAT image of 50%-CuN bonded wafer pair, (c) pull test results of wafer level bonded Cu, 30%-CuN passivation and 50%-CuN passivation.

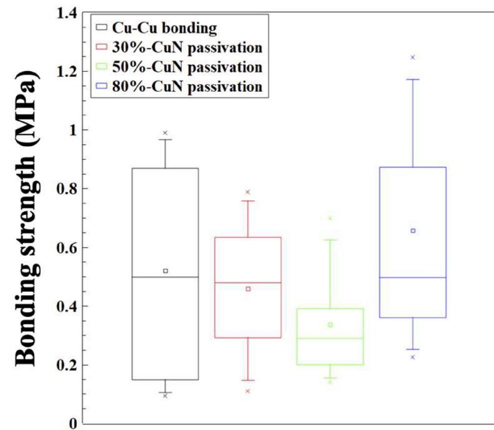

FIGURE 11. Pull test results of chip level bonded Cu, 30%-CuN passivation, 50%-CuN passivation and 80%-CuN passivation.

TABLE 2. Comparison with different low temperature bonding methods.

	Ref. [22]	Ref. [12]	Ref. [15]	This work
Method for low temperature bonding	nt-Cu	Noble metal passivation	CuN by two-step plasma	CuN by PVD
Bonding temperature	150°C	< 100°C	260°C	250°C
Advantage	Higher compatibility with damascene process	Low temperature bonding	Simple surface pretreament	Sequential metal deposition process
Disadvantage	Delicate deposition process	Higher process cost	Influence on topography during CuN formation [20]	Weaker anti-oxidation ability

passivation layer offers higher bonding strength compared to Cu-Cu bonding without any additional pretreatment process.

Based on the SAT image in Fig. 10(b), some voids are still visible in the 50%-CuN passivation specimens. As the bonding condition depends on the CuN decomposition reaction, during wafer level bonding, the generated N_2 gas can become trapped at the bonding interface once the wafer edges are bonded. To address this issue, one possible solution is to reduce the formation of CuN. However, it is crucial to delicately adjust the composition of the flow rate during the deposition process to ensure the anti-oxidation ability is maintained.

The pull test results of chip level bonding specimens with PVD-deposited CuN passivation are presented in Fig. 11. The bonding area for these specimens is approximately 10 x 10 mm. The smaller bonding area facilitates the escape of N_2 byproduct from the bonding interface. As a result, the 80%-CuN passivation specimen was successfully bonded, demonstrating higher bonding strength compared to the 30%- and 50%-CuN specimens.

IV. CONCLUSION

This study demonstrates the feasibility of using PVD-deposited CuN as a low-cost passivation material for low-temperature Cu-Cu bonding. The bonding process leverages the thermal decomposition reaction of CuN, which has been examined and discussed. XRD analysis confirms that the decomposition reaction primarily takes place within the temperature range of 200°C∼250°C. TEM analysis reveals the presence of Cu grains at the bonding interface of CuN-CuN, indicating the connection of Cu atoms from the two bonding pairs when N atoms are expelled during annealing at 250°C.

Properties of the CuN thin film are influenced by the deposition process parameters. When the flow rate of N_2 gas accounts for 30% of the total flow rate, a weaker CuN peak is observed compared to the specimens with 50% and 80% N_2 flow rates. Conversely, the 80%-CuN specimen encountered bonding failure at the wafer level bonding, potentially due to an excessive generation of N_2 gas. Hence, it is crucial to carefully select the deposition parameters based on specific packaging scenarios.

A comparison between PVD-deposited CuN and other methods for low temperature Cu bonding is summarized in Table 2. Despite the bonding temperature of 250°C used in this study not being considered aggressive for low temperature bonding, the use of PVD-deposited CuN offers a relatively simpler process flow and lower process cost. Moreover, it has been reported that the decomposition temperature of CuN varies depending on the deposition approach [19]. In conclusion, based on the demonstrated feasibility of using CuN as passivation for Cu, it indicates the potential for achieving lower bonding temperature requirements by making further adjustments to the thin film properties of CuN.

REFERENCES

[1] R. Mahajan et al., "Embedded multi-die interconnect bridge (EMIB)—A high density, high bandwidth packaging interconnect," in *Proc. IEEE 66th Electron. Compon. Technol. Conf. (ECTC)*, Las Vegas, NV, USA, May 2016, pp. 557–565, doi: 10.1109/ECTC.2016.201.

[2] G. Duan et al., "Advanced substrate packaging technologies for enabling heterogeneous integration (HI) applications," in *Proc. Int. Electron Devices Meeting (IEDM)*, San Francisco, CA, USA, Dec. 2022, pp. 3.4.1–3.4.4, doi: 10.1109/IEDM45625.2022.10019355.

[3] M.-F. Chen, F.-C. Chen, W.-C. Chiou, and D. C. H. Yu, "System on integrated chips (SoIC(TM) for 3D heterogeneous integration," in *Proc. IEEE 69th Electron. Compon. Technol. Conf. (ECTC)*, Las Vegas, NV, USA, May 2019, pp. 594–599, doi: 10.1109/ECTC.2019.00095.

[4] S. W. Liang, G. C. Y. Wu, K. C. Yee, C. T. Wang, J. J. Cui, and D. C. H. Yu, "High performance and energy efficient computing with advanced SoIC^{TM} scaling," in *Proc. IEEE 72nd Electron. Compon. Technol. Conf. (ECTC)*, San Diego, CA, USA, May 2022, pp. 1090–1094, doi: 10.1109/ECTC51906.2022.00176.

[5] X. F. Brun, J. Burggraf, B. Ruxandra-Aida, and C. Muhlstatter, "Low temperature direct bonding of SiN and SiO interfaces for packaging applications," in *Proc. IEEE 70th Electron. Compon. Technol. Conf. (ECTC)*, Orlando, FL, USA, Jun. 2020, pp. 182–187, doi: 10.1109/ECTC32862.2020.00041.

[6] K. Sakuma et al., "Plasma activated low-temperature die-Level direct bonding with advanced wafer dicing technologies for 3D heterogeneous integration," in *Proc. IEEE 71st Electron. Compon. Technol. Conf. (ECTC)*, San Diego, CA, USA, Jun. 2021, pp. 408–414, doi: 10.1109/ECTC32696.2021.00075.

[7] J. Jourdon, S. Lhostis, S. Moreau, P. Lamontagne, and H. Frémont, "Search for copper diffusion at hybrid bonding interface through chemical and electrical characterizations," *Microelectron. Rel.*, vol. 126, Nov. 2021, Art. no. 114217, doi: 10.1016/j.microrel.2021.114217.

[8] M. Chang et al., "Si–H bond breaking induced retention degradation during packaging process of 256 Mbit DRAMs with negative wordline bias," *IEEE Trans. Electron Devices*, vol. 52, no. 4, pp. 484–491, Apr. 2005, doi: 10.1109/TED.2005.844743.

[9] Y. I. Kim, K. H. Yang, and W. S. Lee, "Thermal degradation of DRAM retention time: Characterization and improving techniques," in *Proc. IEEE Int. Rel. Phys. Symp.*, Phoenix, AZ, USA, 2004, pp. 667–668, doi: 10.1109/RELPHY.2004.1315442.

[10] C. S. Tan, D. F. Lim, X. F. Ang, J. Wei, and K. C. Leong, "Low temperature CuCu thermo-compression bonding with temporary passivation of self-assembled monolayer and its bond strength enhancement," *Microelectron. Rel.*, vol. 52, no. 2, pp. 321–324, Feb. 2012, doi: 10.1016/j.microrel.2011.04.003.

[11] M. Lykova et al., "Characterization of self-assembled monolayers for Cu Cu bonding technology," *Microelectron. Eng.*, vol. 202, pp. 19–24, Dec. 2018, doi: 10.1016/j.mee.2018.09.008.

[12] Z.-J. Hong et al., "Room temperature Cu-Cu direct bonding using wetting/passivation scheme for 3D integration and packaging," in *Proc. IEEE Symp. VLSI Technol. Circuits (VLSI Technol. Circuits)*, Honolulu, HI, USA, Jun. 2022, pp. 387–388, doi: 10.1109/VLSITechnologyandCir46769.2022.9830175.

[13] Z.-J. Hong et al., "Investigation of bonding mechanism for low-temperature Cu–Cu bonding with passivation layer," *Appl. Surface Sci.*, vol. 592, Aug. 2022, Art. no. 153243, doi: 10.1016/j.apsusc.2022.153243.

[14] H. Kuwae, K. Yamada, T. Kamibayashi, W. Momose, S. Shoji, and J. Mizuno, "Low-temperature quasi-direct copper–copper bonding with a thin platinum intermediate layer prepared by atomic layer deposition," *Trans. Japan Inst. Electron. Packag.*, vol. 13, pp. 1–9, Jan. 2020, doi: 10.5104/jiepeng.13.E19-014-1.

[15] H. Park, H. Seo, Y. Kim, S. Park, and S. E. Kim, "Low-temperature (260 °C) solderless Cu–Cu bonding for fine-pitch 3-D packaging and heterogeneous integration," *IEEE Trans. Compon. Packag. Manuf. Technol.*, vol. 11, no. 4, pp. 565–572, Apr. 2021, doi: 10.1109/TCPMT.2021.3065531.

[16] H. Seo, H. Park, and S. E. Kim, "Comprehensive analysis of a Cu nitride passivated surface that enhances Cu-to-Cu bonding," *IEEE Trans. Compon. Packag. Manuf. Technol.*, vol. 10, no. 11, pp. 1814–1820, Nov. 2020, doi: 10.1109/TCPMT.2020.3024998.

[17] G. Zhang, Z. Lu, J. Pu, G. Wu, and K. Wang, "Structure and thermal stability of copper nitride thin films," *Indian J. Mater. Sci.*, vol. 2013, pp. 1–6, Dec. 2013, doi: 10.1155/2013/725975.

[18] R. Gonzalez-Arrabal, N. Gordillo, M. S. Martin-Gonzalez, R. Ruiz-Bustos, and F. Agulló-López, "Thermal stability of copper nitride thin films: The role of nitrogen migration," *J. Appl. Phys.*, vol. 107, no. 10, May 2010, Art. no. 103513, doi: 10.1063/1.3369450.

[19] A. Jiang, M. Qi, and J. Xiao, "Preparation, structure, properties, and application of copper nitride (Cu_3 N) thin films: A review," *J. Mater. Sci. Technol.*, vol. 34, no. 9, pp. 1467–1473, Sep. 2018, doi: 10.1016/j.jmst.2018.02.025.

[20] T.-H. Hung et al., "TSV integration with chip level TSV-to-pad Cu/SiO_2 hybrid bonding for DRAM multiple layer stacking," *IEEE Electron Device Lett.*, vol. 44, no. 7, pp. 1176–1179, Jul. 2023, doi: 10.1109/LED.2023.3279828.

[21] L. Hu, S. C. K. Goh, S. Wu, and C. S. Tan, "Sputtered copper nitride-copper nitride direct bonding," in *Proc. IEEE 7th Int. Workshop Low Temperature Bonding 3D Integr. (LTB-3D)*, Nara, Japan, Oct. 2021, pp. 23–23, doi: 10.1109/LTB-3D53950.2021.9598450.

[22] C.-M. Liu et al., "Low-temperature direct copper-to-copper bonding enabled by creep on (111) surfaces of nanotwinned Cu," *Sci. Rep.*, vol. 5, no. 1, p. 9734, May 2015, doi: 10.1038/srep09734.